bioRxiv preprint doi: https://doi.org/10.1101/2022.06.01.494224; this version posted June 3, 2022. The copyright holder for this preprint (which was not certified by peer review) is the author/funder, who has granted bioRxiv a license to display the preprint in perpetuity. It is made available under aCC-BY-NC-ND 4.0 International license.

Main Manuscript for

Inter-regional delays fluctuate in the human cerebral cortex

Joon-Young Moon[1]*, Kathrin Müsch[1], Charles E. Schroeder[2], Taufik A. Valiante[3], and Christopher J. Honey[1]

[1]Dept. of Psychological and Brain Sciences, Johns Hopkins University, Baltimore, MD 21218

[2]Translational Neuroscience Lab Division, Nathan S. Kline Institute for Psychiatric Research,

Orangeburg, NY 10962

[3]Department of Surgery, University of Toronto, Toronto, ON M5T 1P5, Canada

*Corresponding author: Joon-Young Moon

Email: joon.young.moon@gmail.com

Author Contributions: J.-Y.M. and C.J.H. designed research; J.-Y.M. and C.J.H. performed research; J.-Y.M., K.M., and C.J.H. analyzed data; J.-Y.M. performed modeling; J.-Y.M., K.M., C.E.S., and C.J.H. wrote the paper; and T.A.V. supported the data acquisition.

Competing Interest Statement: The authors declare no competing interest.

Preprint Server: The manuscript was deposited as a preprint in bioRxiv. This article is distributed under Creative Commons Attribution-NonCommercial-NoDerivatives License 4.0 (CC BY-NC-ND): Anyone can share this material, provided it remains unaltered in any way, this is not done for commercial purposes, and the original authors are credited and cited.

Classification: Biological sciences; neuroscience

Keywords: ECoG; brain rhythms; brain networks; auditory narrative; cerebral cortex

This PDF file includes:

Main Text
Figures 1 to 5

bioRxiv preprint doi: https://doi.org/10.1101/2022.06.01.494224; this version posted June 3, 2022. The copyright holder for this preprint (which was not certified by peer review) is the author/funder, who has granted bioRxiv a license to display the preprint in perpetuity. It is made available under aCC-BY-NC-ND 4.0 International license.

Abstract

Electrophysiological studies suggest that the excitability fluctuations that underlie oscillatory field potentials can regulate the flow of information between regions. However, most studies of these oscillatory processes have focused on local (circuit-level) changes; less is known about how millisecond-scale inter-regional couplings change with global (cortex-wide) oscillatory states. Therefore, we measured ongoing changes in global oscillations and inter-regional coupling by recording intracranially from the human cerebral cortex. In the presence of an ongoing auditory narrative stimulus, we observed that global increases in low-frequency power (4-14Hz) were associated with stronger and more delayed couplings between regions. Conversely, increases in broadband high-frequency power (65+ Hz) were associated with weaker inter-regional couplings and more frequent zero-lag coupling between regions. Latency changes were predicted both by local oscillatory power (at each site) and by global oscillatory power (averaged across the lateral cerebral cortex). Fluctuations in coupling latency were weakly locked to the auditory stimulus: when we repeated the same narrative, a small number of temporal lobe sites exhibited reliable latency patterns across repetitions. The empirical findings were recapitulated in an amplitude-and-phase coupled oscillator model, in which the increases in latency arose from increases in the effective influence of nodes upon one another. Altogether, gradual and widespread increases in low-frequency oscillations were associated with delayed cortico-cortical couplings in the human brain. These changes in inter-regional latency indicate a shift in the timing of peak excitability between regions; we interpret them in relation to bottom-up and top-down information flow, regulated by nonspecific ascending projections to the cortex.

Significance Statement

Each patch of the cerebral cortex is anatomically connected to many others, but the couplings between regions continually shift as we act, think and perceive. How do ongoing fluctuations in neuronal excitability (as reflected in neural oscillations) affect the couplings between brain regions? Studying intracranial electrophysiological measurements from the human brain during extended external stimulation, we found that increases in low-frequency power (4-14Hz) were associated with stronger, yet more delayed couplings between regions, while increases in high-frequency power (65+ Hz) showed the opposite effect. These changes in inter-regional latency were weakly locked to changes in an external auditory stimulus. Our computational models suggested that increases in latency could be explained by global increases in the effective influence of inter-regional cortico-cortical signaling. Altogether, these data indicate that inter-regional signal flow is highly dynamic, that it changes with the strength of oscillatory processes, and can be weakly locked to an external stimulus. These coupling dynamics may reflect a cortex-wide modulation of the relative influence of top-down and bottom-up signals in the human cerebral cortex.

bioRxiv preprint doi: https://doi.org/10.1101/2022.06.01.494224; this version posted June 3, 2022. The copyright holder for this preprint (which was not certified by peer review) is the author/funder, who has granted bioRxiv a license to display the preprint in perpetuity. It is made available under aCC-BY-NC-ND 4.0 International license.

Introduction

Although each patch of the cerebral cortex is anatomically connected to many others, the couplings between regions continually shift as we act, think and perceive. Electrophysiological studies have indicated that fluctuations in cortical excitability, as indexed by field potential oscillations, can regulate the flow of information along specific brain pathways (1–3) and can affect upcoming behavior (4, 5). However, little is known about how the millisecond-scale couplings between brain regions are related to global oscillatory fluctuations in the human cerebral cortex. Therefore, we set out to measure changes in inter-regional coupling recorded in intracranial electrophysiological measurements from the human brain. We asked: how does the strength and latency of couplings between regions change with oscillatory power? We focused on the delays (latencies) between field potentials in different regions because if fluctuation in the electrical potential in one brain area leads that in another area, then this affects the likelihood that spikes in one area will elicit spikes in the other (6–9). More generally, patterns of zero-lag and nonzero-lag coupling are associated with distinct functional states (10–15).

Intracranial recordings from the human brain have revealed a large-scale pattern of latencies, in which parietal regions often lead temporal regions (8, 16, 17). Some of these latency patterns reflect the occurrence of 4-14 Hz waves traveling along the human cortical surface (17). Pioneering studies in the cerebral cortex of the cat indicated that the delays between brain regions became longer when the animals switched from a task-period to a rest period, and that this shift in delays was accompanied by an increase in alpha-band (10Hz) oscillations (10). Therefore, we hypothesized that, super-imposed on a default pattern of parietal-to-temporal flow, the inter-regional delays would continually fluctuate in the human brain, becoming longer when low-frequency oscillatory processes were stronger. We tested this hypothesis by measuring the inter-regional delays in intracranial recordings from human participants listening to minutes of natural narrative speech.

We found that increases in low-frequency power (4-14 Hz oscillations, LF power) were associated with longer conduction latencies between regions and stronger inter-regional correlations overall. Thus, increases in low-frequency power, both locally (at each recording electrode) and globally (averaged across the lateral cerebral cortex), were associated with a shift from zero-lag coupling to nonzero-lag (delayed) corticocortical coupling. In a small number of sites, the time-varying changes in inter-regional delays could be reliably elicited by presenting a time-varying auditory stimulus; however, the bulk of the latency fluctuations we observed did not show reliable locking to external drivers, and appeared to be endogenously controlled.

To gain insight into the neurophysiological processes that may underlie these changes in inter-regional delay, we modeled the dynamics as a system of phase-and-amplitude coupled oscillators. Our formal model accounted for the data in the following way: when the dynamical influence between regions is increased (e.g. via diffuse neuromodulation or thalamocortical signaling that changes the coupling gain) the amplitude of low-frequency oscillations increases, as does the magnitude and the latency of inter-regional correlations.

These data reveal an organization principle between the mesoscopic and macroscopic dynamics in the human brain: more desynchronized neuronal populations couple to other populations more weakly and with shorter delays, while more synchronized cortical populations couple to other regions more strongly and with longer delays. We consider this set of findings in terms of prior work proposing a role for ascending neuromodulatory projections which regulate arousal, as well as the balance between top-down and bottom-up information flow (18–21).

bioRxiv preprint doi: https://doi.org/10.1101/2022.06.01.494224; this version posted June 3, 2022. The copyright holder for this preprint (which was not certified by peer review) is the author/funder, who has granted bioRxiv a license to display the preprint in perpetuity. It is made available under aCC-BY-NC-ND 4.0 International license.

Results

Latencies fluctuate

Inter-channel latencies were identified using the cross-correlations of the raw voltage traces measured from subdural ECoG electrodes. We analyzed data from 10 participants as they listened to auditory narratives (2 presentations of a 7min 19s stimulus, Table S1 for participants' information). For each channel pair, we computed the cross-correlation of the voltage signal in 2-second sliding windows (Fig. 1*A*). Within each time window, we defined the time lag, τ, as the time-delay associated with maximal inter-electrode correlation (Fig. 1*B*, see Methods). The cross-correlograms and τ values varied over time, as illustrated by an example pair in auditory pathway along the superior temporal gyrus (Fig. 1*C*, mean τ = 5.14 +/- 6.30 ms).

Inter-channel latencies increase with low-frequency oscillatory amplitude

Our initial investigation of electrodes in the auditory pathway identified many sites in which latencies were longer during increase of low-frequency (4-14 Hz) power and were shorter during increases of high-frequency broadband (65+ Hz) power (Fig. 2*B*). For example, for a neighboring electrode-pair in the superior temporal gyrus (STG, Fig. 2), alpha-band (10 Hz) power in those electrodes within a 2s time window was positively correlated with the inter-electrode latency for that window (Spearman ρ = 0.55, $p<<0.01$), while broadband power was negatively correlated with the latency (Spearman ρ = -0.36, $p<<0.01$). Therefore, we set out to characterize the relationship between low-frequency (LF) oscillations strength and inter-regional delays across the lateral cerebral cortex.

The relationship between inter-channel latency and low-frequency power was observed across the parietal, temporal and peri-Rolandic cortex (Fig. 3*A*). Because latencies can only be reliably estimated for regions which exhibit coupling in their dynamics, we focused on "stable channel pairs", which were defined as sites within 25 mm of one another which exhibited peak Pearson cross correlations > 0.3 for 80% of the time windows. Using the stable channel pairs, we then estimated the "latency flow" across the cortical surface by spatially and temporally averaging the vectors of flow between stable pairs (see Methods). Comparing the latency flow for the time windows with the top 10% and bottom 10% of global alpha power (alpha power averaged across all channels), it is apparent that inter-channel latencies and inter-channel correlations increased with alpha power (Fig. 3*A*, left, longer latencies indicated by larger arrows, stronger correlations indicated by warmer colors). Similar results are observed for all low-frequency bands (*SI Appendix* Fig. S1-S3, Table S2). This latency effect was confirmed for each of the 10 participants individually (t-test comparing latencies for top 10% power and bottom 10% power, all p's < 0.05 individually), while the correlation strength effect was present in 8 of the participants. We observed a complimentary (and opposite) effect for high-frequency broadband power (65 + Hz): the inter-channel latencies decreased as global broadband power increased (Fig. S4, Table S2).

Consistent with prior reports (16, 17), we observed that that most flow arrows pointed anterior-inferior in the temporal and parietal lobes, indicating that parietal and posterior temporal dynamics were time-advanced relative to anterior and inferior temporal sites (*SI Appendix* Fig. S5-S6). Of the 8 participants whose coverage included the temporal lobe, 7 exhibited mean flow angles < π/2 radians relative to the posterior-anterior axis along the Sylvian Fissure.

Having found that global flow patterns differed between the smallest and largest oscillation magnitudes (Fig. 3*A*), we next tested the latency changes at the level of individual pairs of electrodes across all values of oscillation magnitude. For each channel pair, we computed the Spearman correlation between

bioRxiv preprint doi: https://doi.org/10.1101/2022.06.01.494224; this version posted June 3, 2022. The copyright holder for this preprint (which was not certified by peer review) is the author/funder, who has granted bioRxiv a license to display the preprint in perpetuity. It is made available under aCC-BY-NC-ND 4.0 International license.

the latency and the global LF power across time windows. We aggregated these values across channel pairs to generate a distribution of correlations. For every participant, the distribution had a positive mean (Fig. 3*B*, Channel Pair Analysis, mean of subject-wise mean Spearman ρ = 0.10), indicating a consistent positive correlation between channel pair latency and the global LF power. This phenomenon was observed for nearest neighbor channel pairs (distance < 12.5 mm, Fig. 3*B*, red) and for next nearest neighbor channel pairs (12.5mmm < distance 25 mm, Fig. 3*B*, blue). Similar results were obtained when we estimated oscillation magnitude using the local LF power nearby each pair of channels, rather than the global LF power averaged across channels (see Methods). Finally, taking a more spatially averaged view, we observed that the mean latency across all electrodes increased within time windows with greater global LF power (Fig. 3*B*, mean latency analysis, mean Spearman ρ = 0.37).

These measurements indicate that the relationship between latency and oscillation amplitude was robust and consistent across measurement methods. Note that it was not possible to test this relationship within electrodes whose couplings were transient or weak (inter-electrode r < 0.3, making up 42% of nearest neighbor channel pairs and 83% of next-nearest neighbor channel pairs), because it was not possible to reliably estimate the inter-electrode delays in such electrodes.

Inter-channel correlations increase with low-frequency oscillatory amplitude

In parallel with the latency effects described above, we also observed that higher amplitude LF power was associated with larger inter-electrodes correlations. This effect is qualitatively apparent in Fig. 3*A*, where greater correlation magnitude (warmer arrow colors) were observed for the higher levels of LF power (left column). Quantitatively, the histogram of correlations between LF-power and inter-channel correlation were positively shifted for all participants (Fig. 3*C*, channel pair analysis, mean Spearman ρ = 0.20 when correlating LF power and coupling magnitude) and the spatial mean of the inter-channel correlation also increased with the LF power (Fig. 3*C*, mean Spearman ρ = 0.45). Once again, the effects associated with LF power were very similar when measured with globally averaged LF power and with the LF power specific to a channel pair (*SI Appendix* Fig. S7). Moreover, these effects also persisted when we included next-nearest neighbor electrode pairs (Fig. 3*B*, *C*).

Stronger oscillations are associated with fewer zero-lag couplings

Did the changes in latency also corresponded to a shift away from isochronous (zero-lag) synchronization? On the one hand, LF power changes might covary with a shift in non-zero delays (e.g. a shift from 5 to 10 ms latency), but on the other hand, LF power changes may covary with a shift from an isochronous synchrony to a lagged synchrony (e.g. from 0ms to 5 ms latency), with distinct functional implications (15). Defining zero-lag as any inter-regional coupling with a latency estimated in the range [-2, 2] msec, we found (in all participants individually) that increases in LF power were associated with decreases in the number of zero-lag pairs (*SI Appendix* Fig. S8). Thus, as LF power increased, the absolute number of zero-lag couplings decreased, even while the number of coupled pairs increased.

Latency fluctuations are weakly locked to the stimulus in the auditory pathways

Given that fluctuations in cortical oscillations can be reliably locked to an auditory narrative stimulus (22, 23), can the inter-regional latency patterns also be locked to an auditory narrative? To answer this question, we first identified pairs of channels which both exhibited a consistent LF power time course across repeats of the narrative stimulus. For example, the channels highlighted in Fig. 2*A* exhibited reliable single-trial LF fluctuations across repeats. For these channels, we defined the *latency reliability* as the correlation between latency values in corresponding 2s windows for run 1 and run 2 of the auditory

bioRxiv preprint doi: https://doi.org/10.1101/2022.06.01.494224; this version posted June 3, 2022. The copyright holder for this preprint (which was not certified by peer review) is the author/funder, who has granted bioRxiv a license to display the preprint in perpetuity. It is made available under aCC-BY-NC-ND 4.0 International license.

stimulus (Fig. 4*B*, *C*). For this pair, we observed that *latency reliability* (Spearman ρ = 0.24 across run 1 and 2), was lower than *LF power reliability* (defined as the Spearman correlation between LF power values in corresponding 2s windows for run 1 and run 2) in channel X (Spearman ρ = 0.66 across run 1 and 2) or channel Y (ρ = 0.45).

Latency reliability was low even in sites entrained to the auditory stimulus, suggesting that fluctuations in latency were more strongly controlled by endogenous processes than by our auditory narrative. For each channel pair with measurable latencies, we compared the latency reliability of that pair against its *LF power reliability* (Spearman correlation between LF power time courses for run 1 and run 2) and its *broadband power reliability* (defined similarly). Across all 10 participants, the latency reliability and LF power reliability were only weakly related (Fig. 4*D*, Spearman ρ = 0.17; individual participant LF and broadband data in *SI Appendix* Fig. S9 and S10). We found that 12% of the pairs yielded LF power reliability greater than 0.2, and 25% exhibited broadband power reliability greater than 0.2, but less than 5% of the pairs yielded the corresponding levels of reliability in their latency time courses. The pairs exhibiting both reliability in LF time courses and in latency patterns were mostly located in in early auditory pathways of the superior temporal cortex.

A coupled oscillator model identifies inter-node influence as key parameter

To probe possible mechanisms underlying the relationships between latencies and global oscillation patterns, we constructed a cortical network model. The model was composed of 78 nodes linked according to inter-regional connections in the human brain (24) (Fig. 5*A*). We employed Stuart-Landau oscillators to represent the neural mass activity at each node, because these oscillators follow the normal form of the Hopf bifurcation, providing the simplest model that captures the amplitude and phase dynamics of neural systems near a bifurcation point (25, 26). The dynamics of each node in the model arise from a combination by (i) intrinsic phase and amplitude dynamics determined by the natural frequency and amplitude assigned to each node and (ii) inter-node influences from anatomically connected neighbors. We fixed the parameters of the intrinsic dynamics, drawing the natural frequencies for each node from a Gaussian distribution with mean of 10 Hz and s.d. of 1 Hz. We varied the coupling strength, S, which globally determines the magnitude of each node's influence on its anatomical neighbors, between S = 0 (no coupling) and S > 1 (very strong coupling).

For intermediate values of the inter-node influence, 0.4<S<1, we observed a match to the empirical phenomenon: there was a positive correlation between the mean latency across nodes, the mean peak cross correlation, and the mean oscillatory amplitudes (Fig. 5*B*). When the inter-node influence (modelled via the coupling strength S) was near zero, the nodes exhibited a uniform distribution of relative phases, because their dynamics were independent. Thus, for S near zero, there was approximately zero correlation between the dynamics of neighboring nodes over many cycles. For strong coupling strengths (S > 1) the nodes became tightly locked with each other over entire cycles and pulled one another into zero-lag synchrony. Thus, strong coupling was associated with decreased latency and increased correlation between network neighbors. However, in the intermediate range of coupling values (0.4<S<1), the oscillators became phase-locked for only a portion of each oscillation cycle, and with non-zero phase difference. In this range, the mean inter-node latency increased with S, as larger values of S within this range were associated with a larger proportion of time spent phase-locked within each cycle.

What other classes of models might explain the experimentally observed correlation between latency and low-frequency power? Moving towards more abstracted models, with less biological connection, the phenomenon can be explained by models that posit a change in the relative magnitude of delayed and

bioRxiv preprint doi: https://doi.org/10.1101/2022.06.01.494224; this version posted June 3, 2022. The copyright holder for this preprint (which was not certified by peer review) is the author/funder, who has granted bioRxiv a license to display the preprint in perpetuity. It is made available under aCC-BY-NC-ND 4.0 International license.

simultaneous inter-node couplings (details in *SI Appendix* Text). For example, we considered a generic model composed of two time series processes, each time series expressed as the sum of two processes: a common process (coupled with a fixed zero delay) and an oscillatory process (coupled across sites with a fixed nonzero delay). As we increase the amplitude of the coupled oscillatory process, the observed inter-regional latency and the oscillatory power will increase in tandem (*SI Appendix* Text, Fig. S11). This simplified model can be understood as an abstraction of the Stuart-Landau model processes (Fig. 5). However, regardless of whether the latency shifts arise from the Stuart-Landau mechanisms (an increase in inter-regional global coupling) or via this more abstracted model, the neurobiological outcome does not change: moments of peak excitability shift from zero-lag to nonzero-lag as low-frequency oscillations increase.

Discussion

Recording intracranially from the human cerebral cortex, we observed that increases in low-frequency power (4-14Hz, especially 6-10Hz) were associated with stronger and more delayed couplings between regions. In time windows when high-frequency broadband power (65+ Hz) was increased we observed the opposite effect: weaker inter-regional couplings and a larger proportion of zero-lag coupling. These changing coupling patterns were observed across the lateral cerebral cortex and were associated with both locally and globally-measured oscillatory processes. Moreover, the increases and decreases in coupling latency were mostly endogenous: when we repeated the same auditory speech stimulus, only a small number of auditory-locked sites exhibited reliable latency patterns across repetitions. Using computational models composed of amplitude-and-phase-coupled oscillators, we found that the empirical changes in coupling magnitude and latency could be explained by increases and decreases in the effective cortico-cortical influence.

What are the functional consequences of the continual waxing and waning of low-frequency oscillatory processes in the human brain? When oscillations are stronger, this is often associated with a decrease in perceptual sensitivity and an increase in the relative strength of long-range communication(27) and perhaps top-down signaling in particular(28, 29). Indeed, low-frequency oscillations have been linked to an idling state and “maintaining the status quo”(30, 31). Here, we show that not only are stronger oscillations associated with stronger coupling between brain regions, but we also find that stronger oscillations are associated with longer delays between regions. Thus, when oscillations are weaker, the couplings are weaker and synchronous; when oscillations are stronger, the couplings are stronger and delayed. Indeed, when the oscillations are especially strong, then many nearby sites may exhibit a shift to a lagged coupling state, and this may manifest in the form of traveling waves across the cortical surface (17, 32, 33).

Our amplitude-and-phase based model can be understood as a generalization of the phase-based model proposed by Zhang et al., 2018 to account for cortical traveling waves. Zhang et al. (2018) showed how traveling waves could be generated by gradients of intrinsic frequencies across a lattice-like cortical sheet. Our model can produce the same traveling wave effects, but it leads to two further predictions. First, our model predicts that continuous changes in the amplitude of the oscillations are related to continuous changes in latency, even in the absence of gradients of intrinsic frequency. Secondly, our model indicates that a node’s degree (number of connections) will influence whether it leads or lags its neighbors (Woo et al., 2021).

What are the functional implications of coordinated shifts between zero-lag and delayed couplings? The topographies of flow were somewhat variable across participants, consistent with the reports of Zhang et

bioRxiv preprint doi: https://doi.org/10.1101/2022.06.01.494224; this version posted June 3, 2022. The copyright holder for this preprint (which was not certified by peer review) is the author/funder, who has granted bioRxiv a license to display the preprint in perpetuity. It is made available under aCC-BY-NC-ND 4.0 International license.

al. (2018), but there were some reliable patterns. In particular, when LF oscillations were strong within the temporal-parietal auditory pathways, the field potentials in higher stages of processing (parietal and posterior temporal cortex) were time-advanced relative to more peripheral regions of the auditory pathway (middle superior temporal cortex) (Fig. 3 and *SI Appendix* Fig. S1-S2). If we assume that there is a "preferred potential" at which the excitability of cortico-cortical projections is increased (13, 34), and that inter-regional axonal conduction delays are 5-10ms (35), then the oscillations will modulate the effectiveness of signaling between regions. For example, when 10 Hz oscillations are elevated, leading to a 5-10 ms time-lead (Fig. 3), then the peak excitability phase of higher order regions will generate spikes that arrive at the peak excitability phase of the low-order regions. Conversely, in the same state, spikes arising from the peak excitability phase of lower-order regions will arrive after the peak excitability phase of the higher order regions. Thus, increases in low-frequency oscillations could increase the relative strength of top-down signaling in the human brain, consistent with theoretical and empirical recordings from non-human primates (28, 36).

We hypothesize that the changes in cortico-cortical delays observed here, in conjunction with changes in oscillatory power, are regulated by spatially nonspecific ascending projections. These signals could arise from controllers of physiological arousal or from nonspecific thalamocortical projections. First, a nonspecific regulation is consistent with the observation that the latency between cortical regions was not only increased in relation to the alpha power in those regions, but also with non-local alpha power measured centimeters away (Fig. 3). Second, we observed only a weak association between the latency patterns and properties of the auditory stimulus that was presented. Third, arousal changes are known to regulate the same oscillatory processes that we measured here (18, 19). Fourth, multi-second latency changes coupled to physiological arousal have been reported in humans using fMRI (21), and latency changes in cats have been observed in relation to spontaneous changes in their attentive state, attributed to ascending modulatory projections (10). Finally, our mathematical model was able to account for the changes in latency via a global (nonspecific) modulation of coupling strength.

Altogether, the data and models suggest that human cortical dynamics reliably transition between near-zero latency states (associated with suppression of alpha-band power and stronger broadband high-frequency power) and longer latency states (associated with increases of alpha-band power and decreases in high-frequency broadband power). The latency changes were observed in widespread temporal, parietal and somatomotor sites; thus, these delay-fluctuations may be associated with distinct large-scale functional states. Although oscillations have been proposed to have multiple roles in organizing cortical communication, the present findings emphasize the importance of slow fluctuations in the amplitude of these oscillations, which appear to mediate transitions between states of latency and dynamical flow across the surface of the human brain. These slow fluctuations may correspond to the large-scale neural state changes observed using fMRI (37, 38).

Two primary limitations of this work are, firstly, that we have not yet mapped the latency fluctuations across a wider range of cognitive and perceptual tasks; and secondly, that we have access to only a subset of brain regions from a clinical population. In relation to the range of stimuli and task states: a natural next step would be to measure these transitions in a sustained attention or vigilance task (4, 39–41), or in the kinds of state-transitions tasks which are associated with gradual large-scale network transitions in neuroimaging (42–44). In relation to the fact that these recordings are from epilepsy patients with coverage primarily in temporal, parietal and peri-Rolandic cortices: these findings may be detectable within a wider range of areas in a neurotypical population using sensor-space analysis of high-density EEG. At the same time, given the earlier report of latency state transitions in the cat brain (10), it may be equally fruitful to search for latency state-transition in rodent or nonhuman primate brains, where high-

bioRxiv preprint doi: https://doi.org/10.1101/2022.06.01.494224; this version posted June 3, 2022. The copyright holder for this preprint (which was not certified by peer review) is the author/funder, who has granted bioRxiv a license to display the preprint in perpetuity. It is made available under aCC-BY-NC-ND 4.0 International license.

resolution recording technologies will make it possible to identify the connection to modulations of the underlying firing rates (45).

Materials and Methods

Detailed descriptions of the materials analyzed, and methods applied are given in *SI Appendix*, Methods.

Acknowledgments

The authors gratefully acknowledge the support of the National Institutes of Mental Health (grant R01MH119099 to C.J.H.; grant R01 MH111439 to C.E.S. with subaward to C.J.H.) and the Alfred P. Sloan Foundation (research fellowship to C.J.H.) as well as the Toronto General and Toronto Western Hospital Foundation. The authors would also like to thank Victoria Barkley for assistance with data collection; David Groppe for support with the iElvis toolbox; and to the staff of the epilepsy monitoring unit at Toronto Western Hospital for logistical support. Finally, our great thanks to the patients who participated in this study.

bioRxiv preprint doi: https://doi.org/10.1101/2022.06.01.494224; this version posted June 3, 2022. The copyright holder for this preprint (which was not certified by peer review) is the author/funder, who has granted bioRxiv a license to display the preprint in perpetuity. It is made available under aCC-BY-NC-ND 4.0 International license.

References

1. T. J. Buschman, E. K. Miller, Shifting the spotlight of attention: evidence for discrete computations in cognition. *Front. Hum. Neurosci.* **4**, 194 (2010).

2. P. Lakatos, *et al.*, Global dynamics of selective attention and its lapses in primary auditory cortex. *Nat Neurosci* **19**, 1707–1717 (2016).

3. M. J. Dahl, M. Mather, M. Werkle-Bergner, Noradrenergic modulation of rhythmic neural activity shapes selective attention. *Trends in Cognitive Sciences* **26**, 38–52 (2022).

4. S. Palva, J. M. Palva, New vistas for α-frequency band oscillations. *Trends in Neurosciences* **30**, 150–158 (2007).

5. J. Samaha, B. R. Postle, The Speed of Alpha-Band Oscillations Predicts the Temporal Resolution of Visual Perception. *Current Biology* **25**, 2985–2990 (2015).

6. M. N. O'Connell, A. Falchier, T. McGinnis, C. E. Schroeder, P. Lakatos, Dual mechanism of neuronal ensemble inhibition in primary auditory cortex. *Neuron* **69**, 805–817 (2011).

7. A. M. Bastos, J. Vezoli, P. Fries, Communication through coherence with inter-areal delays. *Current Opinion in Neurobiology* **31**, 173–180 (2015).

8. J. I. Chapeton, R. Haque, J. H. Wittig, S. K. Inati, K. A. Zaghloul, Large-Scale Communication in the Human Brain Is Rhythmically Modulated through Alpha Coherence. *Current Biology* **29**, 2801-2811.e5 (2019).

9. I. Tal, S. Neymotin, S. Bickel, P. Lakatos, C. E. Schroeder, Oscillatory Bursting as a Mechanism for Temporal Coupling and Information Coding. *Frontiers in Computational Neuroscience* **14**, 82 (2020).

10. P. R. Roelfsema, A. K. Engel, P. König, W. Singer, Visuomotor integration is associated with zero time-lag synchronization among cortical areas. *Nature 1997 385:6612* **385**, 157–161 (1997).

11. W. Singer, Neuronal synchrony: a versatile code for the definition of relations? *Neuron* **24**, 49–65 (1999).

12. F. Varela, J. P. Lachaux, E. Rodriguez, J. Martinerie, The brainweb: Phase synchronization and large-scale integration. *Nature Reviews Neuroscience* **2**, 229–239 (2001).

13. P. Fries, A mechanism for cognitive dynamics: Neuronal communication through neuronal coherence. *Trends in Cognitive Sciences* **9**, 474–480 (2005).

14. P. J. Uhlhaas, *et al.*, Neural synchrony in cortical networks: history, concept and current status. *Front Integr Neurosci* **3** (2009).

15. L. L. Gollo, C. Mirasso, O. Sporns, M. Breakspear, Mechanisms of Zero-Lag Synchronization in Cortical Motifs. *PLoS Computational Biology* **10**, e1003548 (2014).

16. J. I. Chapeton, S. K. Inati, K. A. Zaghloul, Stable functional networks exhibit consistent timing in the human brain. *Brain : a Journal of Neurology* **140**, 628–640 (2017).

bioRxiv preprint doi: https://doi.org/10.1101/2022.06.01.494224; this version posted June 3, 2022. The copyright holder for this preprint (which was not certified by peer review) is the author/funder, who has granted bioRxiv a license to display the preprint in perpetuity. It is made available under aCC-BY-NC-ND 4.0 International license.

17. H. Zhang, A. J. Watrous, A. Patel, J. Jacobs, Theta and Alpha Oscillations Are Traveling Waves in the Human Neocortex. *Neuron* **98**, 1269-1281.e4 (2018).

18. M. J. McGinley, *et al.*, Waking State: Rapid Variations Modulate Neural and Behavioral Responses. *Neuron* **87**, 1143–1161 (2015).

19. D. A. McCormick, D. B. Nestvogel, B. J. He, Neuromodulation of Brain State and Behavior. *https://doi.org/10.1146/annurev-neuro-100219-105424* **43**, 391–415 (2020).

20. E. A. K. Jacobs, N. A. Steinmetz, A. J. Peters, M. Carandini, K. D. Harris, Cortical State Fluctuations during Sensory Decision Making. *Current Biology* **30**, 4944-4955.e7 (2020).

21. R. v. Raut, *et al.*, Global waves synchronize the brain's functional systems with fluctuating arousal. *Science Advances* **7** (2021).

22. C. J. Honey, *et al.*, Article Slow Cortical Dynamics and the Accumulation of Information over Long Timescales. *Neuron* **76**, 423–434 (2012).

23. S. Haufe, *et al.*, On the interpretation of weight vectors of linear models in multivariate neuroimaging. *Neuroimage* **87**, 96–110 (2014).

24. G. Gong, *et al.*, Mapping anatomical connectivity patterns of human cerebral cortex using in vivo diffusion tensor imaging tractography. *Cerebral Cortex* **19**, 524–536 (2009).

25. F. C. (Frank C. Hoppensteadt, E. M. Izhikevich, Weakly connected neural networks. 400 (1997).

26. E. M. Izhikevich, Dynamical Systems in Neuroscience: The Geometry of Excitability and Bursting. *Dynamical Systems in Neuroscience* (2006) https:/doi.org/10.7551/MITPRESS/2526.001.0001 (January 19, 2022).

27. M. Siegel, T. H. Donner, A. K. Engel, Spectral fingerprints of large-scale neuronal interactions. *Nature Reviews Neuroscience* **13**, 121–134 (2012).

28. T. van Kerkoerle, *et al.*, Alpha and gamma oscillations characterize feedback and feedforward processing in monkey visual cortex. *Proc Natl Acad Sci U S A* **111**, 14332–14341 (2014).

29. M. T. Sherman, R. Kanai, A. K. Seth, R. van Rullen, Rhythmic Influence of Top-Down Perceptual Priors in the Phase of Prestimulus Occipital Alpha Oscillations. *J Cogn Neurosci* **28**, 1318–1330 (2016).

30. J. Mo, Y. Liu, H. Huang, M. Ding, Coupling between visual alpha oscillations and default mode activity. *Neuroimage* **68**, 112–118 (2013).

31. R. J. Compton, D. Gearinger, H. Wild, The wandering mind oscillates: EEG alpha power is enhanced during moments of mind-wandering. *Cognitive, Affective and Behavioral Neuroscience* **19**, 1184–1191 (2019).

32. G. Deco, V. Jirsa, A. R. McIntosh, O. Sporns, R. Kötter, Key role of coupling, delay, and noise in resting brain fluctuations (Proceedings of the National Academy of Sciences of the United States of America (2009) 106, 25 (10302-10307) DOI: 10.1073/pnas.0901831106). *Proc Natl Acad Sci U S A* **106**, 12207–12208 (2009).

bioRxiv preprint doi: https://doi.org/10.1101/2022.06.01.494224; this version posted June 3, 2022. The copyright holder for this preprint (which was not certified by peer review) is the author/funder, who has granted bioRxiv a license to display the preprint in perpetuity. It is made available under aCC-BY-NC-ND 4.0 International license.

33. J. A. Roberts, *et al.*, Metastable brain waves. *Nature Communications* **10** (2019).

34. G. Schalk, A general framework for dynamic cortical function: the function-through-biased-oscillations (FBO) hypothesis. *Frontiers in Human Neuroscience* **9**, 352 (2015).

35. R. Caminiti, *et al.*, Diameter, length, speed, and conduction delay of callosal axons in macaque monkeys and humans: Comparing data from histology and magnetic resonance imaging diffusion tractography. *Journal of Neuroscience* **33**, 14501–14511 (2013).

36. C. J. Honey, E. L. Newman, A. C. Schapiro, Switching between internal and external modes: A multiscale learning principle (2017) https:/doi.org/10.1162/netn_a_00024 (January 19, 2022).

37. R. M. Hutchison, *et al.*, Dynamic functional connectivity: Promise, issues, and interpretations. *Neuroimage* **80**, 360–378 (2013).

38. X. Liu, J. H. Duyn, Time-varying functional network information extracted from brief instances of spontaneous brain activity. *Proc Natl Acad Sci U S A* **110**, 4392–4397 (2013).

39. F. Aoki, E. E. Fetz, L. Shupe, E. Lettich, G. A. Ojemann, Increased gamma-range activity in human sensorimotor cortex during performance of visuomotor tasks. *Clinical Neurophysiology* **110**, 524–537 (1999).

40. W. Klimesch, EEG alpha and theta oscillations reflect cognitive and memory performance: A review and analysis. *Brain Research Reviews* **29**, 169–195 (1999).

41. D. Osipova, *et al.*, Theta and gamma oscillations predict encoding and retrieval of declarative memory. *Journal of Neuroscience* **26**, 7523–7531 (2006).

42. A. Turnbull, *et al.*, Reductions in task positive neural systems occur with the passage of time and are associated with changes in ongoing thought. *Scientific Reports 2020 10:1* **10**, 1–10 (2020).

43. J. Smallwood, *et al.*, The neural correlates of ongoing conscious thought. *iScience* **24** (2021).

44. A. Turnbull, *et al.*, Left dorsolateral prefrontal cortex supports context-dependent prioritisation of off-task thought. *Nat Commun* **10**, 1–10 (2019).

45. L. Muller, F. Chavane, J. Reynolds, T. J. Sejnowski, Cortical travelling waves: mechanisms and computational principles. *Nat Rev Neurosci* **19**, 255 (2018).

bioRxiv preprint doi: https://doi.org/10.1101/2022.06.01.494224; this version posted June 3, 2022. The copyright holder for this preprint (which was not certified by peer review) is the author/funder, who has granted bioRxiv a license to display the preprint in perpetuity. It is made available under aCC-BY-NC-ND 4.0 International license.

Figures

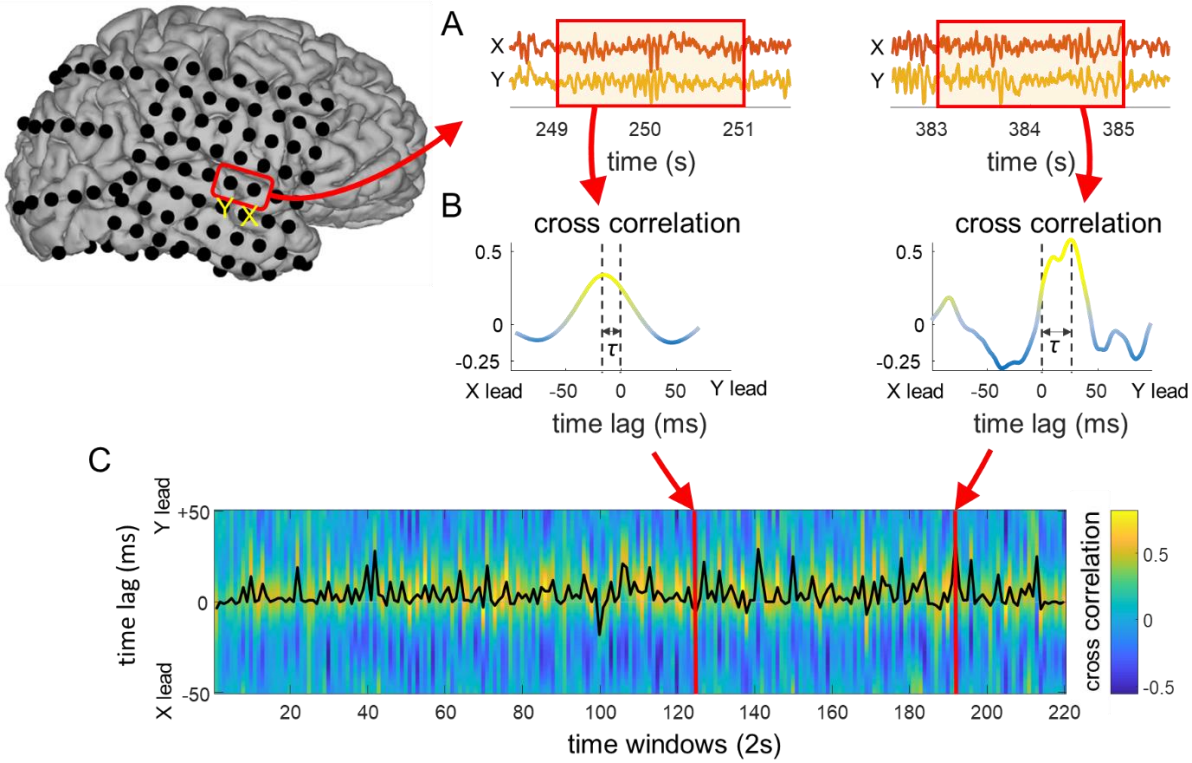

Fig. 1. Schematic of latency analysis. We presented a 7-minute auditory narrative twice to each participant. **(*A*)** Moving time windows were applied to the pair of chosen channels. **(*B*)** Within each time window, we measured the cross correlation between the pair. The latency τ was defined as the time lag yielding the maximum cross-correlation between the channels. **(*C*)** Cross correlation (blue to yellow colors) and latency τ (black line) of this channel pair are illustrated for all time windows. The latency τ fluctuates throughout the time course.

bioRxiv preprint doi: https://doi.org/10.1101/2022.06.01.494224; this version posted June 3, 2022. The copyright holder for this preprint (which was not certified by peer review) is the author/funder, who has granted bioRxiv a license to display the preprint in perpetuity. It is made available under aCC-BY-NC-ND 4.0 International license.

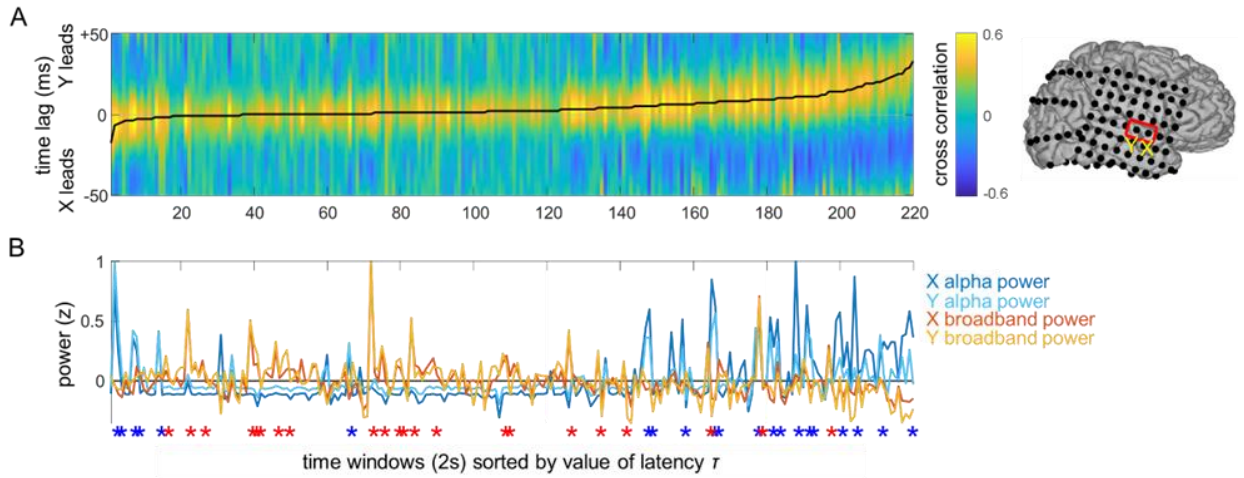

Fig. 2. Latency and power changes for an electrode pair in the middle STG. Time windows are sorted by value of Latency τ between electrodes *X* and *Y*. For each channel pair, we arranged the time windows in the increasing order of the latency *τ*, and measured mean alpha-band (10 Hz) power and mean broadband (65+ Hz) power across channels for each corresponding time window. **(*A*)** Cross correlation between two chosen channels is shown for each time window, sorted by the value of latency *τ*. Black line denotes the inter-electrode latency *τ*. **(*B*)** Alpha-band (7-14Hz) and broadband power in each channel for each 2s time window. Blue asterisks denote alpha peaks and red asterisks denote broadband power peaks (top 10% of values). The latency *τ* is correlated with alpha power and anti-correlated with broadband power.

bioRxiv preprint doi: https://doi.org/10.1101/2022.06.01.494224; this version posted June 3, 2022. The copyright holder for this preprint (which was not certified by peer review) is the author/funder, who has granted bioRxiv a license to display the preprint in perpetuity. It is made available under aCC-BY-NC-ND 4.0 International license.

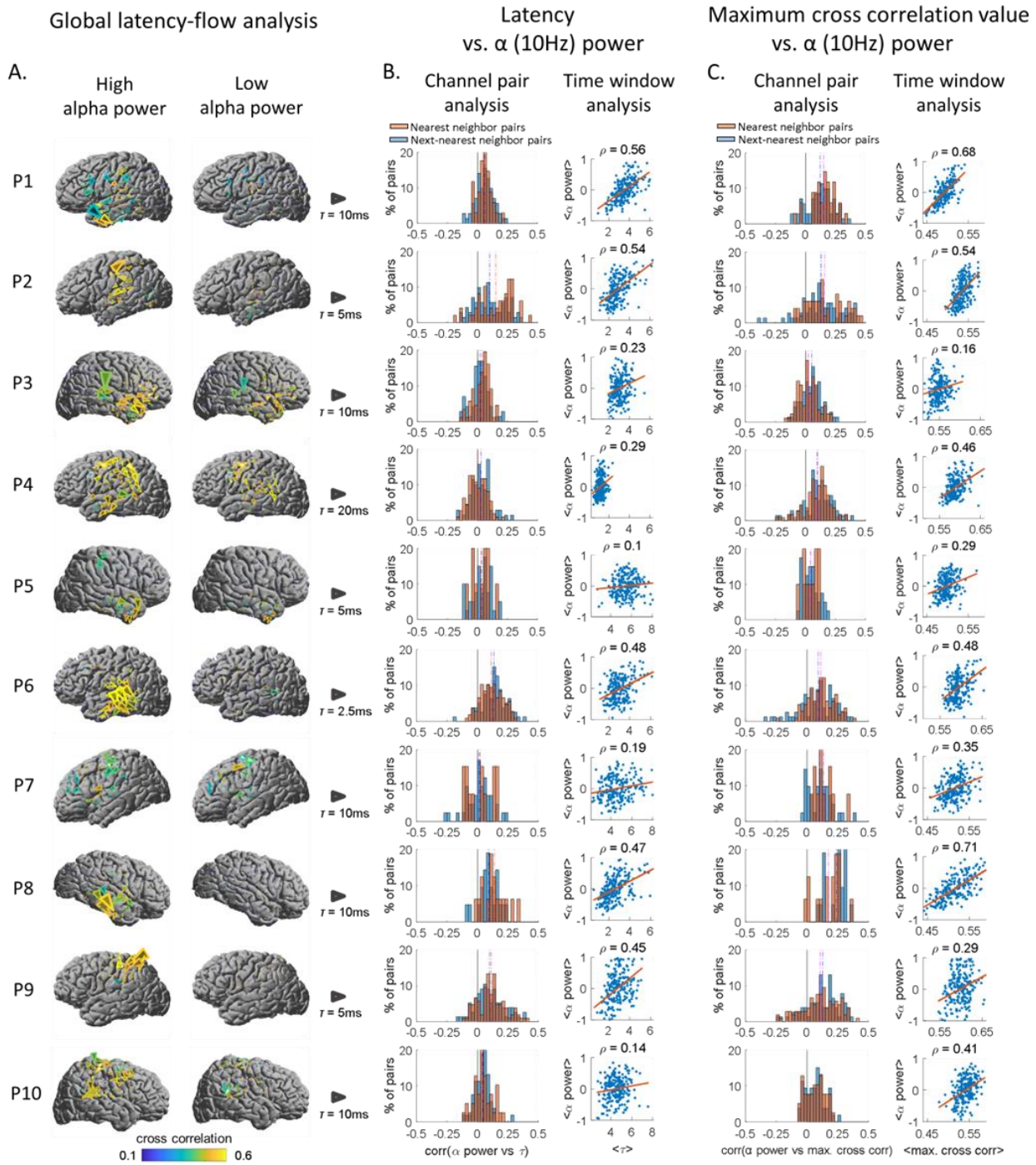

Fig. 3. Latencies and coupling strengths increase with low-frequency power. (*A*) *Global latency-flow analysis.* Latency-flow patterns for high alpha power time windows and low alpha power time windows are shown. Top 10% of the windows yielding highest alpha power and bottom 10% of the windows yielding lowest alpha power are chosen, and latency flows are computed across the chosen windows respectively. Yellower color of arrows denotes higher cross correlation. Larger size of arrows denotes longer latencies. The size of arrows on each flow map is scaled for readability: the grey arrow next to each participant's

bioRxiv preprint doi: https://doi.org/10.1101/2022.06.01.494224; this version posted June 3, 2022. The copyright holder for this preprint (which was not certified by peer review) is the author/funder, who has granted bioRxiv a license to display the preprint in perpetuity. It is made available under aCC-BY-NC-ND 4.0 International license.

brain map denotes scale of latency flow arrows. **(*B*)** *Time delay vs. alpha power.* Channel pair analysis: Correlation between latencies of pairs and global alpha power for each pair across time windows are computed and the distribution is shown in histograms. Red histogram represents nearest neighbor pairs and blue histogram represents next-nearest neighbor pairs. The distribution is positively skewed. Time window analysis: Mean latencies across pairs and mean global alpha power for each time window are computed and shown as scatterplots. The distributions yield positive correlation. **(*C*)** *Maximum cross correlation vs alpha power.* Channel pair analysis: Correlation between maximal cross correlation of pairs and global alpha power for each pair across time windows are computed and the distribution is shown in histograms. The distribution is positively skewed. Time window analysis: Mean maximal cross correlations across pairs and mean global alpha power for each time window are computed and shown as scatterplots. The distributions yield positive correlation.

bioRxiv preprint doi: https://doi.org/10.1101/2022.06.01.494224; this version posted June 3, 2022. The copyright holder for this preprint (which was not certified by peer review) is the author/funder, who has granted bioRxiv a license to display the preprint in perpetuity. It is made available under aCC-BY-NC-ND 4.0 International license.

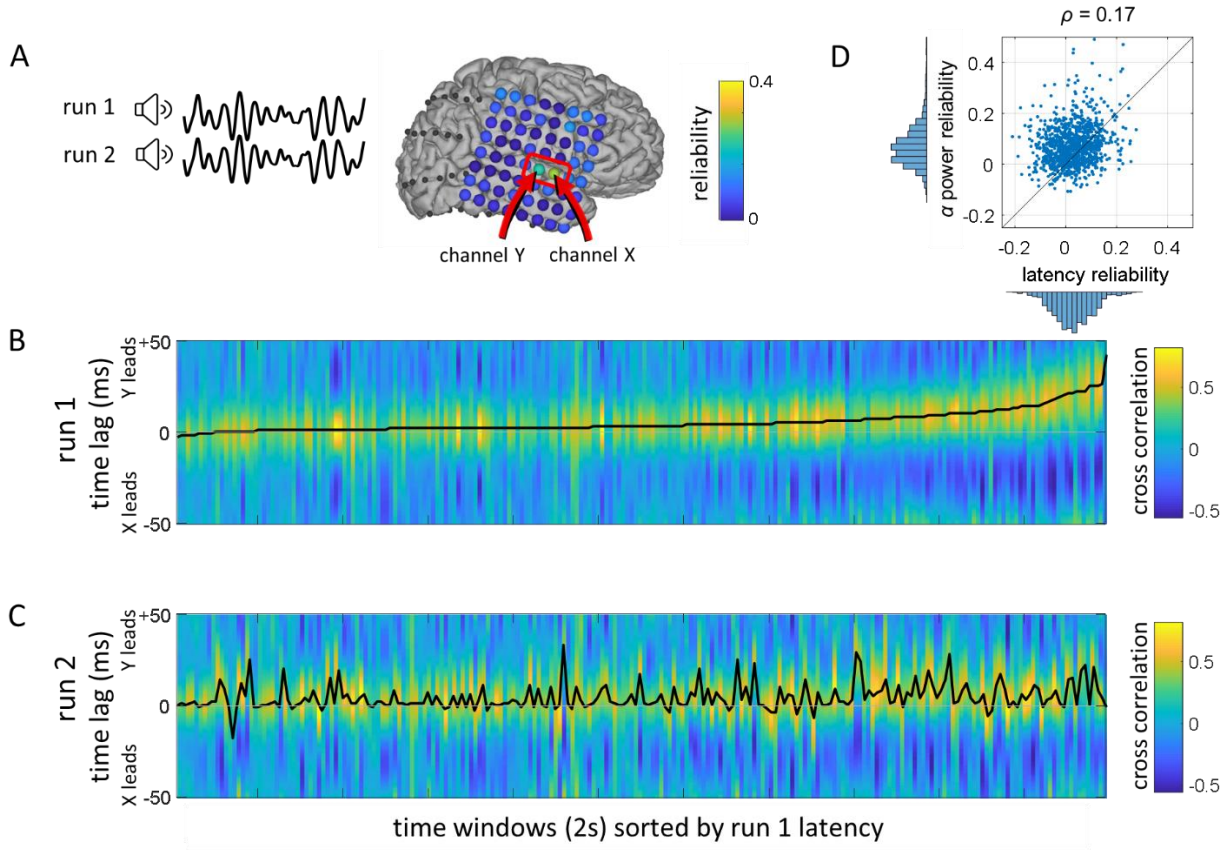

Fig. 4. Reliability of latency patterns between run 1 and run 2. (*A*) Two runs of the same auditory stimulus were applied to a participant., and channels with high reliability between two runs were chosen. **(*B*)** The latency pattern for run 1 is shown in the order of increasing latency. **(*C*)** The latency pattern for run 2 is shown in the same order used in run 1. The latency reliability between two runs was 0.25 for the chosen channel pair. **(*D*)** Latency reliability vs. LF power reliability for all channel pairs from 10 participants.

bioRxiv preprint doi: https://doi.org/10.1101/2022.06.01.494224; this version posted June 3, 2022. The copyright holder for this preprint (which was not certified by peer review) is the author/funder, who has granted bioRxiv a license to display the preprint in perpetuity. It is made available under aCC-BY-NC-ND 4.0 International license.

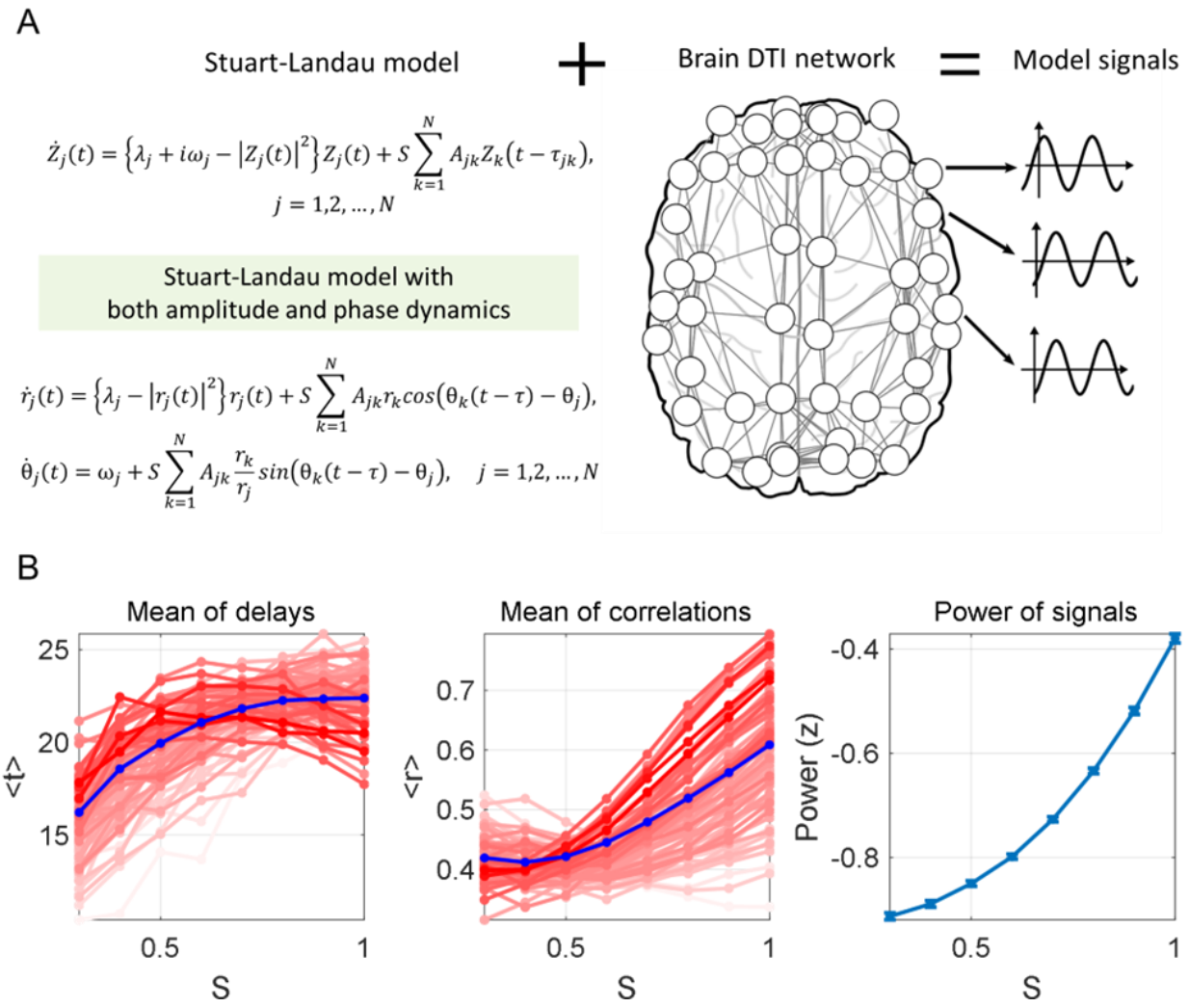

Fig. 5. Coupled oscillator model on brain network. (*A*) Stuart-Landau coupled oscillator model is applied to diffusion tensor imaging (DTI) structural brain network consisting of 78 nodes. **(*B*)** Mean delay across the nodes, mean of maximal cross correlations across the nodes, mean of power of the nodes are shown. Below a certain critical coupling strength S (~1.0), all three measures are positively correlated with each other as the coupling strength S increases.